Journal of Alloys and Compounds 503 (2010) 474–479

Contents lists available at ScienceDirect

Journal of Alloys and Compounds

journal homepage: www.elsevier.com/locate/jallcom

Comparative studies on properties of scandia-stabilized zirconia synthesized by the polymeric precursor and the polyacrylamide techniques

G.C.C. Costa [1], R. Muccillo *

Centro de Ciência e Tecnologia de Materiais, Instituto de Pesquisas Energéticas e Nucleares, C.P. 11049, S. Paulo, SP, 05422-970 Brazil

ARTICLE INFO

Article history:
Received 21 November 2009
Received in revised form 6 May 2010
Accepted 8 May 2010
Available online 20 May 2010

Keywords:
Zirconia–scandia
Powder synthesis
X-ray diffraction
Impedance spectroscopy

ABSTRACT

ZrO_2:Sc_2O_3 powders were synthesized by the polyacrylamide and the polymeric precursor techniques. The powder particles had the state of agglomeration analyzed by laser scattering, the structural phases by X-ray diffraction, and the morphology by scanning electron microscopy. The polyacrylamide and the polymeric precursor techniques produced stable transparent gels and polymeric resins, respectively. Upon calcination the gels and the resins yielded high surface area powders, fully stabilized in the cubic fluorite structure. The crystalline phases, grain morphology and electrical behavior of sintered pellets using powders synthesized by both techniques were analyzed. The amount of organics in the precursors was found to be responsible for the state of agglomeration of the particles, producing pellets with different electrical behavior.

1. Introduction

Solid solutions of zirconium oxide with yttrium, scandium and alkaline earth (calcium and magnesium) oxides are widely reported as suitable solid electrolytes for oxygen sensors and SOFCs (solid oxide fuel cells) due to their high oxide ion conductivity [1]. The most studied of these compounds, yttria-stabilized zirconium oxides, are solid electrolyte components in SOFC devices operating in the 800–1000 °C range. The stabilization, i.e., the formation of the cubic phase stable at temperatures lower than that found in pure zirconium oxide, may be achieved by making solid solutions of this oxide with aliovalent cation (Ca^{2+}, Mg^{2+}, Y^{3+}, Sc^{3+}) oxides. All these ion substitutions promote O^{2-} vacancy formation for charge compensation, and Sc-stabilized ZrO_2 (ScSZ) is the zirconia-based solid electrolyte with the highest ionic conductivity, due to the low association enthalpy of the O^{2-} vacancy with Sc^{3+} ions, and the smallest difference between the Sc^{3+} and Zr^{4+} ionic radii [2]. ZrO_2:Sc_2O_3 has been proposed to be used as solid electrolyte in SOFCs operating at intermediate temperatures (600–800 °C). Its oxide ion conductivity (0.3 S/cm at 1000 °C for ZrO_2:10 mol% Sc_2O_3 – hereafter 10ScSZ) is higher than that of ZrO_2:8 mol% Y_2O_3–8YSZ (0.1 S/cm) [3]. The first Japanese-made 1 kW SOFC system was fabricated using ScSZ sheets as electrolytes with flexibility, high-strength and twice the conductivity of yttria-stabilized zirconia system [4]. ScSZ tapes were obtained by tape casting to prepare multilayer anode-supported SOFCs [5]. Recently, studies on nanostructured single phase ScSZ prepared by mechanochemical synthesis were reported with excellent mechanical properties but unusual electrical behavior [6]. Scandium oxide may be chemically extracted from rare-earth containing monazite sand in Brazil after purification of rare-earth concentrates [7]. Many techniques have been reported to obtain ScSZ ceramic powders, such as co-precipitation [8–11], citrate [10], EDTA-citrate complexing [12], glycine nitrate [13], polymeric precursor [14], spray drying [15], combustion [16] and sol–gel [17]. Most of these techniques are time consuming if large quantities of powders are required.

In this study, ScSZ powders were synthesized by the polymeric precursor technique and for the first time by the polyacrylamide technique. The polyacrylamide technique proceeds via a polymerization reaction that combines an initiator with acrylamide and bisacrylamide (crosslinker agent) to form a gel. This gel consists of long polymeric chains, crosslinked to create a three-dimensional tangled network, soaked with a solution of cations [18]. The polymerization of acrylamide occurs in the following sequence [19,20]: (a) the initiator is decomposed into primary free radicals, which can combine with the monomer molecule to produce monomer-free radicals, which, in turn, can combine with monomers producing chain-free radicals [19–21]; this reaction proceeds continuously and acrylamide (AAm) molecules polymerize into polymer chains; (b) a network is formed with the polymer chains by their cross-linking and bridging between polymer chains by N,N′-methylenebisacrylamide (bis-AAm) molecules reaction; (c)

* Corresponding author. Fax: +55 11 3133 9276.
E-mail address: muccillo@usp.br (R. Muccillo).
[1] Present address: Peter A. Rock Thermochemistry Laboratory and NEAT ORU, University of California at Davis, One shields Avenue, Davis, CA 95616, USA.

0925-8388/$ – see front matter © 2010 Elsevier B.V. All rights reserved.
doi:10.1016/j.jallcom.2010.05.036

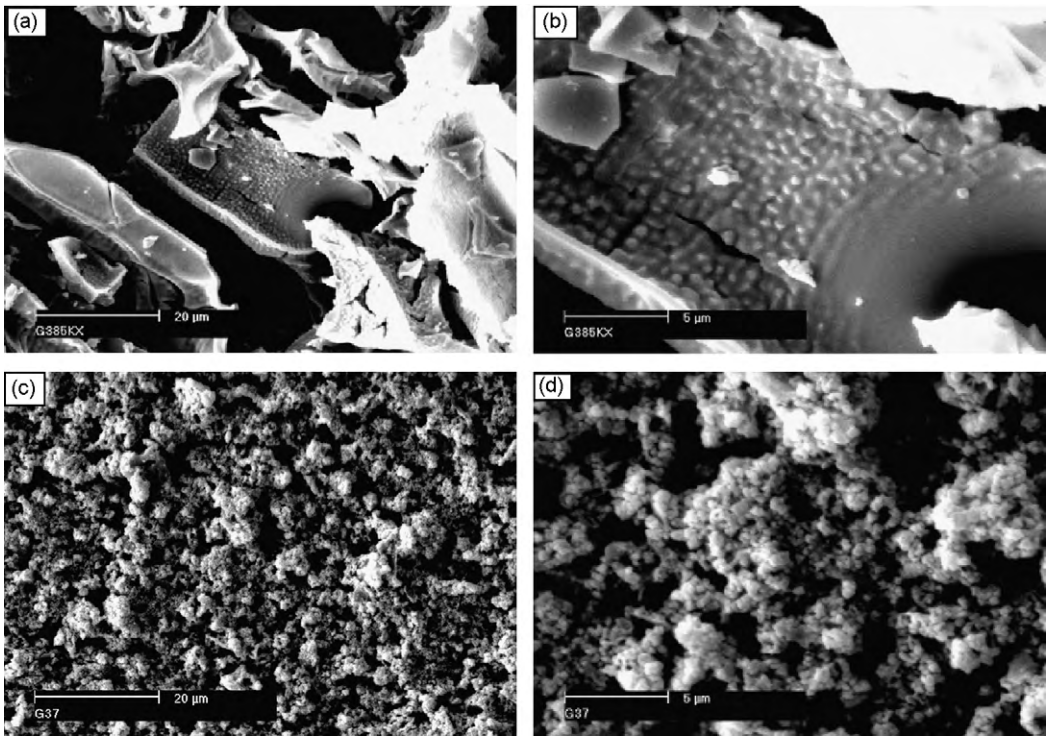

Fig. 1. Scanning electron microscopy images of 10ScSZ powders synthesized by the polymeric precursor technique (a and b) and by the polyacrylamide technique (c and d), calcined at 650 °C for 4 h.

bis-AAm is added into the monomer solution to polymerize the monomers completely. One of the advantages of the polyacrylamide technique is the reproducibility of the batches for obtaining submicron size ceramic powders in large quantities.

The simultaneous (TG and DTA) thermal analysis of the polyacrylamide gel and the precursor solution obtained by the polymeric precursor technique is reported here. The powders obtained from calcination of the gels were analyzed by nitrogen gas adsorption (BET), X-ray diffraction (XRD) and scanning electron microscopy (SEM). The powders were pressed and sintered for further analysis by XRD, SEM and impedance spectroscopy.

2. Experimental

For the synthesis of scandia-stabilized zirconia powders, the starting materials were ZrO_2 produced at this Institute, Sc_2O_3 99.9%, citric acid – $C_6H_8O_7$ 99.5%, ethylene glycol – CH_2OHCH_2OH 99%, HNO_3 65%, acrylamide – C_3H_5NO 98%, ammonium persulfate – $(NH_4)_2S_2O_8$ 98% and N,N′-methylenebisacrylamide – $C_7H_{10}N_2O_2$ 98%, all commercial analytical grade (Alfa Aesar). The ZrO_2 and the Sc_2O_3 compounds were first dissolved separately in hot nitric acid solution under stirring, and the Zr^{4+} and Sc^{3+} cations were complexed by the addition of citric acid (CA) in the 1:1.2 ratio with the pH adjusted (3–5 range) to dissolve completely the species, getting a clear solution. These stock solutions were mixed in the 0.9 Zr^{4+}:0.2 Sc^{3+} molar ratio to obtain the precursor solutions. The experimental procedures for the two synthesis techniques, polyacrylamide and polymeric precursor, are described below in detail:

2.1. The polyacrylamide technique

The monomers of acrylamide (5 g, 70 mmol) and the crosslinker N,N′-methylenebisacrylamide (0.26 g, 1.7 mmol) were dissolved in 100 mL of the precursor solutions. The resulting solutions were heated and continuously stirred during the whole process. When the temperature reached about 65 °C, a small amount (0.04 g, 0.18 mmol) of the ammonium persulfate (APS) initiator was added into the solutions. The solution rapidly polymerized into transparent polymeric gels without any precipitation. The gels were heat treated at 400 °C for 4 h to yield a brownish powder, which was then homogenized in a mortar and calcined at 500 °C up to 650 °C for 4 h.

2.2. The polymeric precursor technique

The precursor solutions were added to ethylene glycol (EG) and citric acid (CA) in the ratio (1 M^{x+}:4CA:16EG) and heated at 90 °C up to 120 °C under stirring to promote the polyesterification reaction. The polymeric solutions were heated at 400 °C for 4 h and the resultant black powders were homogenized in a agate mortar and then calcined at 500 °C up to 650 °C for 4 h.

The calcined resin and the gel were characterized by laser scattering (granulometer 1064, Cilas) to evaluate the particle size distribution, by BET analysis (ASAP 2000, Micromeritics) to determine the surface area, and by scanning electron microscopy (XL 30, Philips) to observe the powder morphology and evaluate the average particle size. The results of the high temperature X-ray diffraction experiments and the determination of average crystallite sizes have already been described [22].

Commercial 10ScSZ powders from DKKK Co., Ltd., Japan, were also used to prepare pellets in a way similar to that used for preparing pellets from 10ScSZ powders synthesized in our laboratories.

The powders were uniaxially pressed at 0.3 MPa, isostatically at 21 MPa and sintered in air at 1600 °C for 1 h. For electrical measurements, colloidal silver was applied to the parallel surfaces of the sintered specimens (disks 10 mm diameter, 1.5 mm thickness) and cured at 200 °C. The impedance spectroscopy measurements were carried out in the 300–550 °C range with a Hewlett–Packard 4192A LF impedance analyzer connected to a HP 362 controller. An inconel 600 sample chamber, with platinum leads and a K-type thermocouple with its junction close to the specimens, was inserted in a programmable Lindberg-BlueM furnace. The $[-Z''(\omega) \times Z'(\omega)]$ impedance spectroscopy data were collected at constant temperature in the 5 Hz to 13 MHz frequency range, 20 pair of values per decade, with an applied ac voltage of 100 mV. A special software was used for collecting and analyzing these data [23].

3. Results and discussion

Scanning electron microscopy images of the as-synthesized ZrO_2:10 mol% Sc_2O_3 powders are shown in Fig. 1.

The powders obtained by the polymeric precursor technique (Fig. 1a and b) consist mainly of small hard agglomerates exhibiting irregular shapes with faceted borders, often lengthened, with average size around 20 μm, similar to the average particle size determined by laser scattering. However, these hard agglomerates consist of sintered nanoparticles resulting from the high-energy environment during thermal decomposition of the large amount

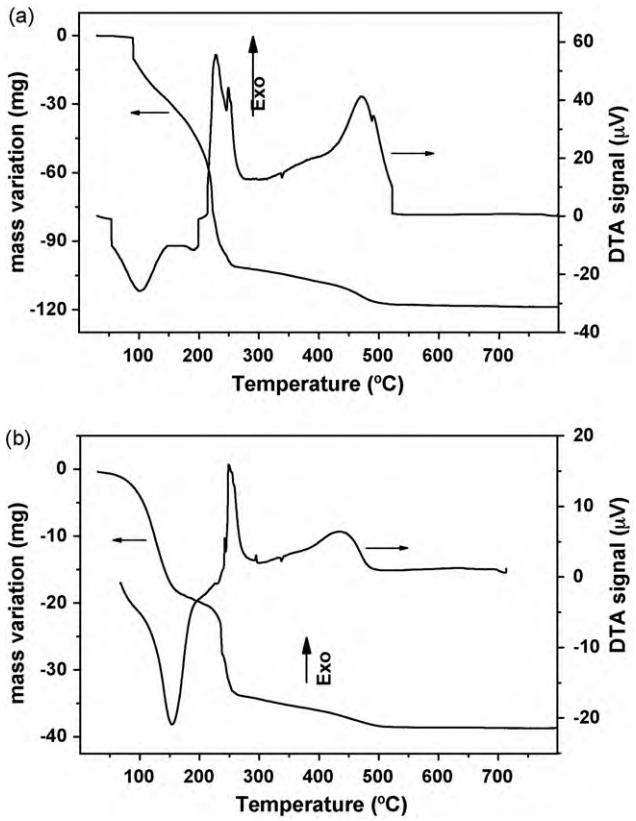

Fig. 2. Thermogravimetric/differential thermal analysis curves of the as-prepared 10ScSZ polymeric resin (a) and polyacrylamide gel (b).

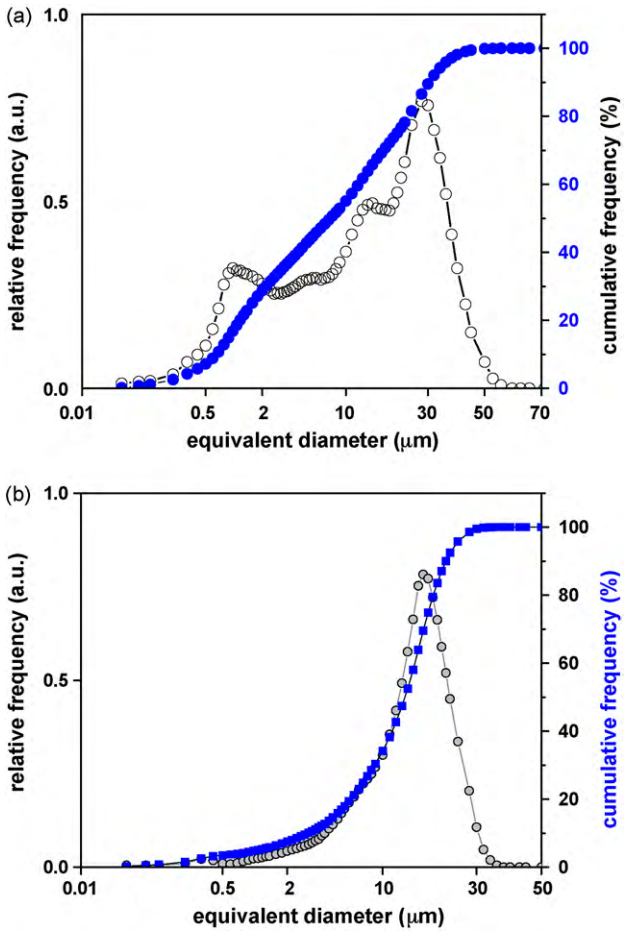

Fig. 3. Relative and cumulative frequency of distribution of particle sizes of 10ScSZ powders prepared by the polyacrylamide (a) and polymeric precursor (b) techniques as-synthesized.

of organic compounds used in the synthesis of the polymeric precursors. The powders obtained by the polyacrylamide technique (Fig. 1c and d), on the other hand, consist mainly of small soft agglomerates of average size around 10 μm and exhibit regular spherical shapes. These agglomerates were not sintered because the content of organic compounds used in the synthesis was relatively low. After heat treatment, we assumed that the particle agglomerates typically follow the morphology established from the precursor solution [24]. In the case of the polyacrylamide technique, it corresponds to the smallest and softest agglomerate with the highest specific surface area. Nevertheless, when preparing ZrO_2:10 mol% Sc_2O_3 powders, there are two conditions that seem to give different powder morphology: (1) it is important to consider the difference in the molecular size of the complexes. In the polyacrylamide technique, the citric acid was used only to complex the metal and no further reaction of polymerization occurred in the remainder reactive carboxylic group. Therefore, the resultant molecule of the complex has straight-chains shorter than the chains produced by the polymeric precursor technique, due to a subsequent esterification and polymerization between the free carboxylic group from citric acid and the free hydroxyl group from ethylene glycol. (2) In the polyacrylamide technique, the addition of low content of organic material into the initial solution required lower calcination temperature.

Fig. 2 shows results of thermal analysis of the 10ScSZ resin resulting from the polymeric precursor technique (2a) and of the gel resulting from the polyacrylamide technique (2b). The two endothermic reactions in Fig. 2a, peaking at 100 °C and at 190 °C, with a corresponding loss of mass in the TG curve, are due to removal of adsorbed water and coordination in the inner sphere; the de-esterification of the polymeric resin has its onset at 230 °C, accompanied by the removal at 250 °C of the respective carboxylic groups along with the mass loss shown in the TG curve [13]; the exothermic process occurring from 310 °C to 470 °C is associated with the full decomposition of the organic polymer [13]. Fig. 2b shows that an endothermic reaction starts at approximately 133 °C along with a mass loss in the TG curve. This endothermic process is due to water removal inside the polymeric network of the gel. The second exothermic reaction at 250 °C, along with the loss of mass, is due to the initial stage of the polyacrylamide decomposition. In this temperature range, ammonia gas is released due to an imidic reaction. A second decomposition range begins at 320 °C, with the decomposition rate reaching its maximum at about 470 °C. This range is assigned to the breakdown of imide groups to nitrile, breakdown of the polymer backbone, and decomposition of the citric acid complex to yield 10ScSZ powders.

Fig. 3 shows the distribution of particle size of 10ScSZ powders synthesized by the polyacrylamide and by the polymeric precursor techniques, Fig. 3a and b, respectively. The distribution in Fig. 3a has many components with a large fraction of particles with average size higher than ~20 μm, while in Fig. 3b the distribution has a main component in the whole measured range with an average particle size of approximately 13 μm. All these values refer to powder agglomerates because these synthesis techniques produce powders with particle size in the submicron range.

To ensure the compositional homogeneity of metal ions and the fuel for combustion during calcination, citric acid is the complexing agent for the two chemical synthesis techniques used in this work; the oxygen in the reaction atmosphere is the oxidizer for the combustion. Therefore, the exothermic reactions of the

Table 1
Values of the average particle size of powders synthesized by the polyacrylamide and the polymeric precursor techniques, as a function of the attritor milling time.

Milling time (min)	Average particle size (μm)	
	Polyacrylamide	Polymeric precursor
0	17.7	15.3
30	2.7	0.9
60	1.4	0.7
90	1.2	0.6

oxidative removal of organic compounds during calcinations at relatively high temperatures (500–650 °C) often transform the weak bonds between particles into sintered necks, producing undesirable agglomeration of the powders. Hence, these agglomerates with 12–30 μm average size obtained by the two techniques may introduce interparticle porosity in the green compacts prepared for sintering. The difference in the distribution of the agglomerate size of powders produced following the two chemical synthesis techniques is due to the different (organic compounds)/(powder) ratio. Therefore, additional quantities of organic compound further produce enough energy to join the particles together during calcination, resulting in agglomerates. The degree of agglomeration of powders obtained by the polymeric precursor technique is higher than that of powders obtained by the polyacrylamide technique due to the relative higher quantities of ethylene glycol and citric acid used in the former synthesis technique. This will result in sintered specimens with larger pore content, and consequently higher electrical resistivity compared to specimens prepared with powders synthesized by the polyacrylamide technique.

The values of specific surface area are further strong evidences of modification of the powders during calcination. Both powders prepared according to the two different techniques have high surface area after calcination at 500 °C: 78 m^2/g and 167 m^2/g for powders synthesized by the polyacrylamide technique and by the polymeric precursor technique, respectively. The values of the specific surface area, in agreement with the particle size distribution, show that the temperature of calcination plays an important role on the final surface area of powders obtained by the polymeric precursor technique. The densification behavior of a powder compact is influenced mainly by the particle size, its distribution and the degree of agglomeration [24]. Therefore, the formation of agglomerates can be a problem when synthesizing ceramic materials. Large agglomerates may be found even in calcined powders with high specific surface area, prepared by the polymeric precursor technique. Milling is usually required to break these agglomerates to obtain dense sintered compacts.

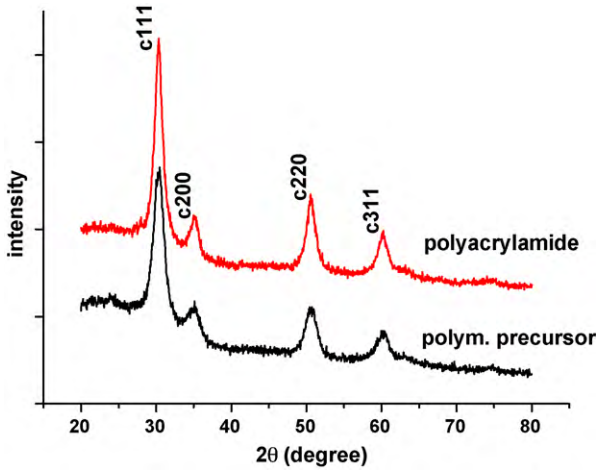

Fig. 4. Room temperature X-ray diffraction patterns of 10ScSZ powders prepared by the polyacrylamide and polymeric precursor techniques after calcination at 400 °C. c: cubic phase.

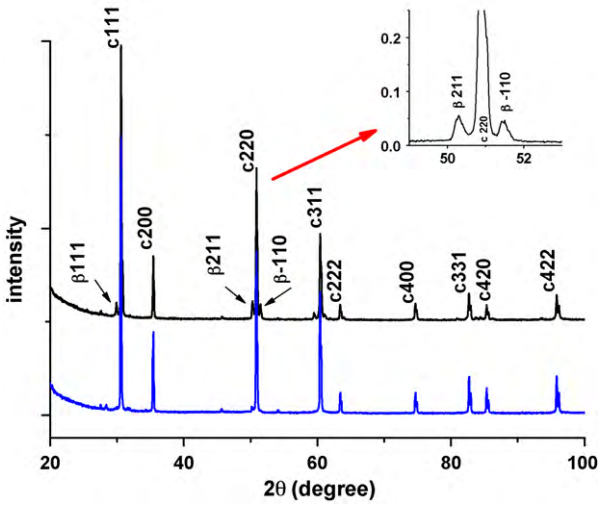

Fig. 5. Room temperature X-ray diffraction patterns of 10ScSZ sintered pellets using powders prepared by the polyacrylamide (bottom) and polymeric precursor (top) techniques. c: cubic phase, β: rhombohedral phase. Inset: zoom of the 49–53° 2θ region.

The powders were milled in an attritor for 30 min, 60 min and 90 min to break up the agglomerated particles. Table 1 shows the results. Milling for 1.5 h was sufficient for obtaining powders with reduced and unimodal distribution of particle size. These milled powders were used for pressing and sintering pellets for X-ray diffraction and electrical analyses.

Fig. 4 shows the results of X-ray diffraction measurements in ScSZ powders synthesized by the two techniques – polyacrylamide and polymeric precursor – and calcined at 400 °C. Both powders crystallize in the cubic fluorite structure with average crystallite size < 10 nm, evaluated with the Scherrer equation [22]. X-ray diffraction analysis of sintered (1600 °C/1 h) pellets prepared with powders synthesized by the polyacrylamide and the polymeric precursor techniques, Fig. 5, shows the cubic fluorite phase. Small amplitude reflections of the rhombohedric phase (inset of Fig. 5) for the pellet prepared with powders synthesized by the polyacrylamide technique are detected [22,25].

Fig. 6 shows impedance spectroscopy diagrams measured at 400 °C in 10ScSZ pellets sintered at 1600 °C, using powders

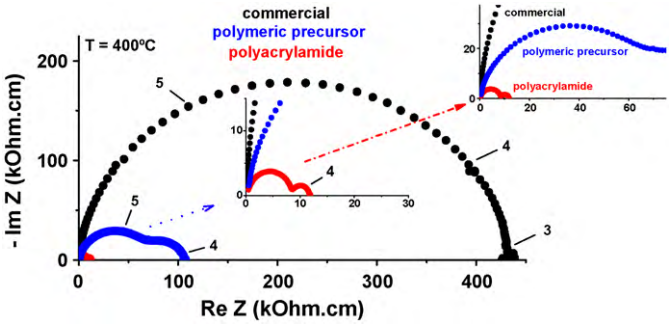

Fig. 6. Impedance spectroscopy diagrams in the 5 Hz to 13 MHz frequency range of 10ScSZ solid electrolyte sintered pellets using powders synthesized by the polyacrylamide and by the polymeric precursor techniques. The diagram of a sintered pellet prepared with a commercial powder is also shown. The numbers indicate the logarithm of the frequency (Hz).

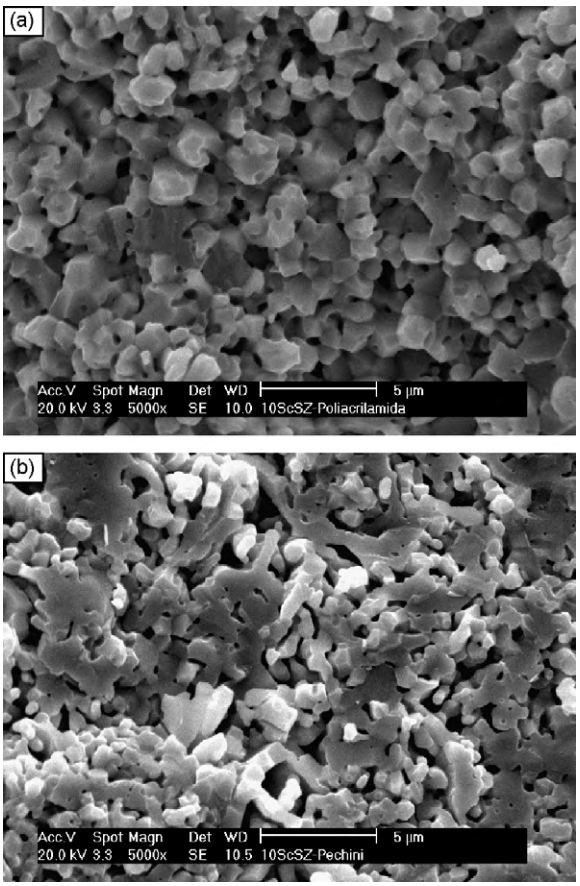

Fig. 7. Scanning electron microscopy images of fracture surfaces of sintered 10ScSZ pellets. (a) using powders synthesized by the polyacrylamide technique; (b) by the polymeric precursor technique.

synthesized by the polyacrylamide technique and by the polymeric precursor technique. The impedance diagram measured in the pellet prepared with commercial powder, sintered at 1600 °C, is also shown. The impedance diagrams of pellets prepared with powders synthesized in our laboratories show two well defined semicircles at high and at low frequencies, due to intragranular (bulk) and intergranular (grain boundary) contributions to the electrical resistivity, respectively. Each semicircle may be represented by an equivalent circuit composed of a resistor in parallel with a constant phase element (CPE) when the center of these semicircles lies below the Z' axis [26]. The impedance of a CPE is given by $Z_{CPE} = Q^{-1}(j\omega)^{-\alpha}$, $0 \leq \alpha \leq 1$ [27]. Z (Ω cm) = $R{\cdot}S/t$, the resistance R (Ω) is determined at the intersection of the semicircles with the x-axis, S (cm^2) is the electrode area and t (cm) is the specimen thickness. Q (F/cm) = $2{\cdot}\pi{\cdot}f_0{\cdot}Z$, f_0 (Hz) is the frequency at the apex of the semicircle. The electrical resistivity/associated CPEs of the bulk (high frequency) of the three specimens measured at 400 °C were evaluated: $1.2 \times 10^4\ \Omega$ cm/6.7×10^{-12} F/cm, $1.1 \times 10^5\ \Omega$ cm/7.9×10^{-12} F/cm and $4.3 \times 10^5\ \Omega$ cm/7.4×10^{-12} F/cm for the polyacrylamide, the polymeric precursor and the commercial pellets, respectively. The specific capacitance values are typical of bulk capacitances of solid electrolytes [28]. Pellets prepared with the commercial powder show relatively larger bulk resistivity and negligible grain boundary resistivity.

Fig. 7 shows images of fracture surfaces of the sintered pellets, using powders synthesized by the polyacrylamide technique and by the polymeric precursor technique. The polyacrylamide pellet has regular shaped grains with an estimated average size 0.3 μm. Intergranular as well as intragranular pores are evident without substantial neck formation between grains, an evidence of minimum intergrain sintering, in agreement with the impedance spectroscopy results (grain boundary semicircle). The polymeric precursor pellet, on the other hand, presents partially sintered irregular shaped grains. They have a large pore volume, also in agreement with the grain boundary semicircle in the impedance diagram. One may consider that the large pore volume and the incomplete intergrain sintering in both pellets are a result of the irregular shape of the agglomerates, which, in turn, are a consequence of the liberation of energy by organic residues during synthesis. That is why commercial powders, synthesized by chemical routes, are usually processed after synthesis [29].

4. Conclusions

The procedure for the synthesis of ZrO_2:10 mol% Sc_2O_3 powders by the polyacrylamide technique is described in detail for the first time. The procedure for the synthesis of the same compounds by the polymeric precursor technique is also described. High values of specific surface area were obtained. The polyacrylamide technique is suitable for producing large quantities of powders. Another advantage is that before calcination for obtaining the powders, the gel may be stored at ambient atmosphere without degradation. The electrical conductivity values, evaluated by impedance spectroscopy measurements, show that the grain boundary conductivity is to a large extent affected by the degree of agglomeration of the synthesized ceramic powder. This agglomeration is found to be due to the relative amount of organics used in the synthesis. The total electrical conductivity of sintered pellets, using different powders, increased according to the sequence: commercial, polymeric precursor and polyacrylamide powders.

Acknowledgements

The authors acknowledge the financial supports of CNEN, FAPESP (Procs. 98/10798-0, 05/53241-9 and 05/54171-4) and CNPq (Proc. 306285/2006-1). They also thank Dr. J.R. Martinelli for measuring particle size distribution, and C.V. Moraes for operating the SEM microscope. The authors gratefully thank Daiichi Kigenso Kagaku Kogyo, Japan, for supplying the commercial powders.

References

[1] B.C.H. Steele, A. Heinzel, Nature 414 (2001) 345–352.
[2] C. Haering, A. Roosen, H. Schichl, M. Schnöller, Solid State Ionics 176 (2005) 261–268.
[3] O. Yamamoto, Y. Arati, Y. Takeda, N. Imanishi, Y. Mizutami, M. Kawai, Y. Nakamura, Solid State Ionics 79 (1995) 137–142.
[4] Y. Mizutani, K. Hisada, K. Ukala, H. Sum, M. Yokoyama, Y. Nakamura, O. Yamamoto, J. Alloys Compd. 408 (2006) 518–524.
[5] Z.R. Wang, J.Q. Qian, H.D. Cao, S.R. Wang, T.L. Wen, J. Alloys Compd. 437 (2007) 264–268.
[6] V.V. Zyryanov, N.F. Uvarov, V.A. Sadykov, A.S. Ulihin, V.G. Kostrovskii, V.P. Ivanov, A.T. Titov, K.S. Paichadze, J. Alloys Compd. 483 (2009) 535–539.
[7] A. Abrão, Química e Tecnologia das Terras Raras, CETEM-CNPq, Rio de Janeiro, Brazil, 1994.
[8] Z. Lei, Q.S. Zhu, Solid State Ionics 176 (2005) 2791–2797.
[9] S.P.S. Badwal, J. Drennan, Solid State Ionics 53–56 (1992) 769–776.
[10] M. Okamoto, Y. Akimune, K. Furuya, M. Hatano, M. Yamanaka, M. Uchiyama, Solid State Ionics 176 (2005) 675–680.
[11] K. Biswas, Ceram. Int. 35 (2009) 2047–2051.
[12] H.X. Gu, R. Ran, W. Zhou, Z.P. Shao, J. Power Sources 172 (2007) 704–712.
[13] D. Lee, I. Lee, Y. Jeon, R. Song, Solid State Ionics 176 (2005) 1021–1025.
[14] Y.W. Zhang, A. Li, Z.G. Yan, G. Xu, C.S. Liao, C.H. Yan, J. Solid State Chem. 171 (2003) 434–438.
[15] F. Tietz, W. Fischer, T. Hauber, G. Mariotto, Solid State Ionics 100 (1997) 289–295.
[16] Z. Lei, Q. Zhu, S. Zhang, J. Eur. Ceram. Soc. 26 (2006) 397–401.
[17] Y. Mizutani, M. Tamura, M. Kawai, O. Yamamoto, Solid State Ionics 72 (1994) 271–275.
[18] A. Sin, P. Odier, Adv. Mater. 12 (2000) 649–652.
[19] T. Tanaka, Sci. Am. 244 (1981) 124.
[20] Q.Q. Tan, M. Gao, Z.T. Zhang, Z.L. Tang, Mater. Sci. Eng. A 382 (2004) 1–7.

[21] A. Ravve, Principles of Polymer Chemistry, Plenum Press, New York, 1995.
[22] G.C.C. Costa, R. Muccillo, Solid State Ionics 179 (2008) 1219–1222.
[23] M. Kleitz, J.H. Kennedy, in: P. Vashishta, J.N. Mundy, G.K. Shenoy (Eds.), Fast Ion Transport in Solids, Elsevier/North-Holland, The Netherlands, 1979, p. 185.
[24] F.F. Lange, J. Am. Ceram. Soc. 67 (1984) 83–89.
[25] H. Fujimori, M. Yashima, M. Kakihana, M. Yoshimura, J. Appl. Phys. 91 (2002) 6493–6498.
[26] G.J. Brug, A.L.G. Van der Eeden, M. Sluyters-Rehbach, J.H. Sluyters, J. Electroanal. Chem. 176 (1984) 275–295.
[27] E. Barsoukov, J. Ross, Macdonald: Impedance Spectroscopy, Theory, Experiment, and Applications, Wiley-Interscience, USA, 2005.
[28] J.G. Fletcher, A.R. West, J.T.S. Irvine, J. Electrochem. Soc. 142 (1995) 2650–2654.
[29] D. Segal, Chemical Synthesis of Advanced Ceramic Materials, Cambridge Univ. Press, Cambridge, UK, 1989.